A DISTRIBUTED-LUMPED-ACTIVE BIQUADRATIC NETWORK FUNCTION REALIZATION

by

L. P. Huelsman

Prepared under Grant NGL-03-002-136
for the Instrumentation Division of
the Ames Research Center, National
Aeronautics and Space Administration

ENGINEERING EXPERIMENT STATION
COLLEGE OF ENGINEERING
THE UNIVERSITY OF ARIZONA
TUCSON, ARIZONA

A Distributed-Lumped-Active Biquadratic

Network Function Realization

Prepared under Grant NGL-03-002-136 for the
Instrumentation Division of the Ames Research Center
National Aeronautics and Space Administration

by

L. P. Huelsman

Department of Electrical Engineering
University of Arizona
Tucson, Arizona

Abstract: This report discusses the use of a simple distributed-lumped-active network configuration which can be used to give a dominant pole approximation to a biquadratic voltage transfer function with complex left-half-plane poles and complex zeros. Design charts and example network realizations are given.

March 1971

A Distributed-Lumped-Active Biquadratic Network Function Realization

This is one of a series of reports describing the use of digital computational techniques in the analysis and synthesis of DLA (Distributed-Lumped-Active) networks. This class of networks consists of three distinct types of elements, namely, distributed elements (modeled by partial differential equations), lumped elements (modeled by algebraic relations and ordinary differential equations), and active elements (modeled by algebraic relations). Such a characterization is especially applicable to a broad class of circuits, especially including those usually referred to as linear integrated circuits, since the fabrication techniques for such circuits readily produce elements which may be modeled as distributed, as well as the more conventional lumped and active ones. The network functions which describe distributed elements, however, involve hyperbolic irrational functions of the complex frequency variable. The complexity of such functions make the use of digital computational techniques most desirable in analyzing and synthesizing these networks.

In this report we shall discuss the use of a DLA network configuration which can be used to approximate a biquadratic voltage transfer function in which the position of the dominant complex-conjugate poles and zeros may be independently adjusted. Such a network function is readily applicable to a broad range of filtering applications. The basic network configuration is shown in Fig. 1. This network configuration was first introduced in a previous report.[1] It consists of a uniform distributed RC element with total resistance R_o and total capacitance C_o, a lumped network element Y_I which may be either a resistor or a capacitor, and an ideal non-inverting voltage controlled voltage source of gain K (indicated by the triangle). For the case where the element labeled Y_I is a capacitor, the voltage transfer function may be shown to be

$$\frac{V_2}{V_1} = \frac{r_f \theta \sinh\theta + R_o}{R_o - R_o\cosh\theta + \frac{1}{K}\{(r_f + \frac{C_I R_o}{C_o})\ \theta\sinh\theta + (R_o + 2C_I r_f R_o p)\cosh\theta - 2C_I r_f R_o p\}} \tag{1}$$

where

$$\theta = \sqrt{R_o C_o p} \tag{2}$$

and p is the complex frequency variable. For the case where Y_I is a resistor the voltage transfer function has the form

$$\frac{V_2}{V_1} = \frac{r_f \theta \sinh\theta + R_o}{R_o - R_o\cosh\theta + \frac{1}{K}\{(r_f + \frac{R_o}{R_I C_o p})\ \theta \sinh\theta + (R_o + \frac{2R_o r_f}{R_I})\cosh\theta - \frac{2R_o r_f}{R_I}\}} \tag{3}$$

It should be noted that the numerator of the above network function is identical with the numerator of the network given in (1) for the case where Y_I is a capacitor.

The network shown in Fig. 1 has five degrees of freedom, namely, the values of the quantities R_o, C_o, r_f, K, and Y_I. Two of these degrees of freedom may be eliminated by making appropriate impedance and frequency normalizations. To do this let us choose values for C_o and R_o such that when r_f is set to unity the network will have a transmission zero on the $j\omega$ at 1 rad/sec. The determination of these values is found by setting the numerator polynomial of (1) or (3) to zero and setting $p = j1$. The solution is the same as that obtained for the distributed-lumped notch network, namely, $R_o = 17.786$ ohms and $C_o = 0.629$ farads. For such normalizations the plot of the dominant locus of the zero of (1) or (3) as a function of the value of r_f is shown in Fig. 2. This chart may be used as a design chart to determine the value of r_f for a desired set of dominant zeros in the normalized transfer function. Now let us consider the realization of the desired dominant pole locations for the network function. From the denominators of (1) and (3) we see that after normalizing R_o and C_o the pole locations will be a function of three network variables, namely, r_f, K, and C_I or R_I. Since there are three variables which interact to determine the normalized pole locations we require a series of charts rather than a single chart to show the relation between these variables and the pole locations. Such a series of charts is shown in Fig. 3-11. These figures show loci of constant K and constant r_f for various values of C_I from 0.7 - 0.05 farads (Figs. 3-7). A similar set of loci for $C_I = 0$, i.e., for R_I = infinity (Fig. 8), and similar sets of loci for values of R_I from 20 - 10 ohms (Figs. 9-11). To meet a given set of design specifications it may, of course, be necessary to interpolate between the various charts shown in Figs. 3-11. If we consider the relative locations of the poles as shown by Figs. 3-11 and zeros as shown in Fig. 2 we conclude that, in general, for high-Q cases network functions in which the pole positions are closer to the origin than the zero positions will require the use of a capacitor for the network element Y_I while network functions for which the pole positions are farther from the origin than the zero positions will require the use of a resistor for the three elements. A design procedure using the charts given in Figs. 2-11 and the necessary frequency normalization is readily formulated as follows.

1. Find the point on the normalized locus shown in Fig. 2 which has the same damping ratio as the upper-half-plane zero in the specified network function which is to be synthesized.

   This determines the value of r_f and also determines the frequency normalization constant ω_n where

$$\omega_n = \frac{\text{real (or imaginary) part of zero to be synthesized}}{\text{real (or imaginary) part of point on locus}} \qquad (4)$$

This assumes $R_o = 17.786$ ohms and $C_o = 0.629$ farads.

2. Frequency normalize the pole locations in the specified network function using the relation

$$p_0' = p_0/\omega_n \tag{5}$$

where p_0 is the original pole location and p_0' is the normalized location.

3. Use the charts shown in Figs. 3-11 to determine the values of K and R_I (or C_I) for the value of r_f found in step 1 above. Interpolate between charts as necessary.

4. Frequency normalize the network by changing the values of all the capacitors using the realization

$$C' = C/\omega_n \tag{6}$$

where C is the value of C_o (or C_I) found in steps 1-3, and C' is the denormalized value.

As an example of the application of this procedure, consider the voltage transfer function

$$\frac{V_2(p)}{V_1(p)} = \frac{(p + .3 + j1.5)\ (p + .3 - j1.5)}{(p + 1.6 + j1.6)\ (p + 1.6 - j1.6)} = \frac{p^2 + .6p + 2.34}{p^2 + 3.2p + 5.12} \tag{7}$$

Applying the procedure defined above to this network function we obtain the following results from each of the steps.

1. The feedback resistor $r_f = 1.9$ ohms. The frequency normalization factor $\omega_n = 2$.
2. The normalized pole locations are $p_0 = -0.8 \pm j0.8$.
3. The family of curves for which the point $(-0.8 + j0.8)$ is on the $r_f = 1.9$ curve is $R_I = 11$, and the gain of

the VCVS is 1.25.

4. The denormalized value of the distributed capacitor C_o is 0.315 farads.

The results obtained by the procedure given above may be improved by using complex optimization[2] in connection with an optimization algorithm such as may be found in the GOSPED optimization package.[3] Applying such a procedure to the preceding example we obtain the following results.

Table 1

Element	Value Found from Design Charts	Value Found by Complex Optimization
r_f	1.9	1.87
R_I	11	10.7
K	1.25	1.22
R_o	17.786	17.96
C_o	0.629	0.633
Error	1.37×10^{-2}	4.80×10^{-11}

Note:

$$\text{Error} = \left| \frac{V_1}{V_2}(p) \right|^2 + \left| \frac{V_2}{V_1}(p) \right|^2$$

$$p = -0.15 + j0.75 \qquad\qquad p = -0.8 + j0.8$$

As an indication of the relative accuracy of the unoptimized (chart determined) network realization and the optimized one, in Figs. 12 and 13, the magnitude and phase curves for the actual network function given in (7), the network whose values were determined directly from the charts, and the network with optimized values, have been plotted.

As a second example of the use of the charts given in Figs. 2-11 consider the following all-pass voltage transfer function

$$\frac{V_2(p)}{V_1(p)} = \frac{(p-.2 + j1.2)\ (p-.2 - j1.2)}{(p+.2 + j1.2)\ (p+.2 - j1.2)} = \frac{p^2 - .4p + 1.48}{p^2 + .4p + 1.48} \tag{8}$$

Applying the steps defined above we obtain the following:

1. The feedback resistor $r_f = 0.54$ ohms. The frequency normalization constant is 0.943.
2. The normalized pole locations are $p_0 = -0.212 \pm j1.272$.
3. Interpolating between Figs. 8 and 9 we obtain $R_I = 100$ ohms and $K = 0.95$.
4. The denormalized value of the distributed capacitance C_o is 0.66 farads.

If we again use these values as a starting point for a complex optimization procedure we obtain the results summarized in the following table.

Table 2

Element	Value Found From Design Charts	Value Found by Complex Optimization
r_f	0.54	0.632
R_f	100	99.42
K	0.943	0.961
R_o	17.786	21.02
C_o	0.629	0.526
Error	5.71×10^{-2}	1.07×10^{-10}

Note:

$$\text{Error} = \left| \frac{V_1}{V_2}(p) \right|^2 + \left| \frac{V_2}{V_1}(p) \right|^2$$

$$p = 0.212 + j1.272 \qquad p = -0.212 + j1.272$$

The magnitude and phase characteristics for the actual network function given in (8), the network whose values are determined directly from the charts and the network whose element values have been optimized are shown in Figs. 14 and 15.

Conclusion

In this report we have presented a series of charts which may be used to synthesize a biquadratic network function with complex poles and zeros by means of a simple DLA network configuration. In addition to their use directly as a design method, the charts have a further advantage in that they may be used to furnish a starting point which optimization procedures can further refine if a more accurate realization of the specified network function is desired.

References

1. Huelsman, L. P., and F. L. Watson, Automated Generation of Distributed-Lumped-Active Network Design Charts by Digital Computer Root-Locus Techniques, University of Arizona, Engineering Experiment Station, Report prepared under NASA Grant NGL-03-002-136, 43 pages, July 1969.

2. Huelsman, L. P., Complex Optimization and Its Application to Distributed-Lumped-Active Networks, University of Arizona, Engineering Experiment Station Report prepared under NASA Grant NGL-03-002-136, 16 pages, March 1970.

3. Huelsman, L. P., GOSPED - A General Optimization Software Package for Electrical Network Design, University of Arizona, Engineering Experiment Station Report prepared under NASA Grant NGL-03-002-136, 94 pages, Sept. 1968.

Acknowledgment

The support of this research by the Instrumentation Division of the Ames Research Center, National Aeronautics and Space Administration, under Grant NGL-03-002-136 is most gratefully acknowledged. The author would also like to acknowledge the assistance of Mr. S. Raghunath who assisted with the computer programming for generating the various design charts presented in this report.

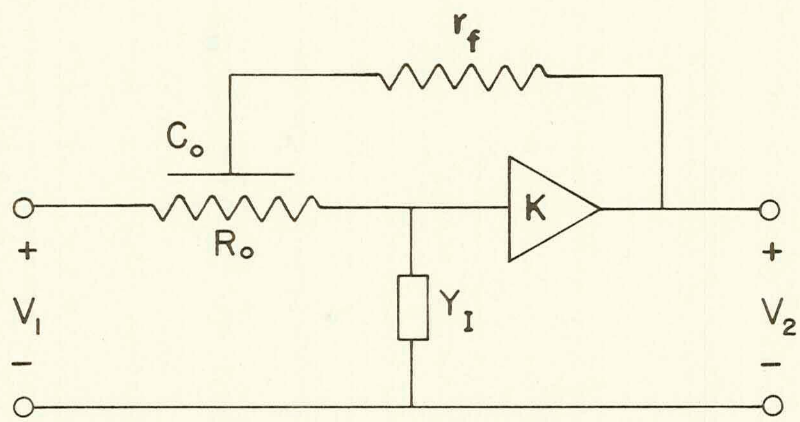

Figure 1 DLA network for biquadratic function realization.

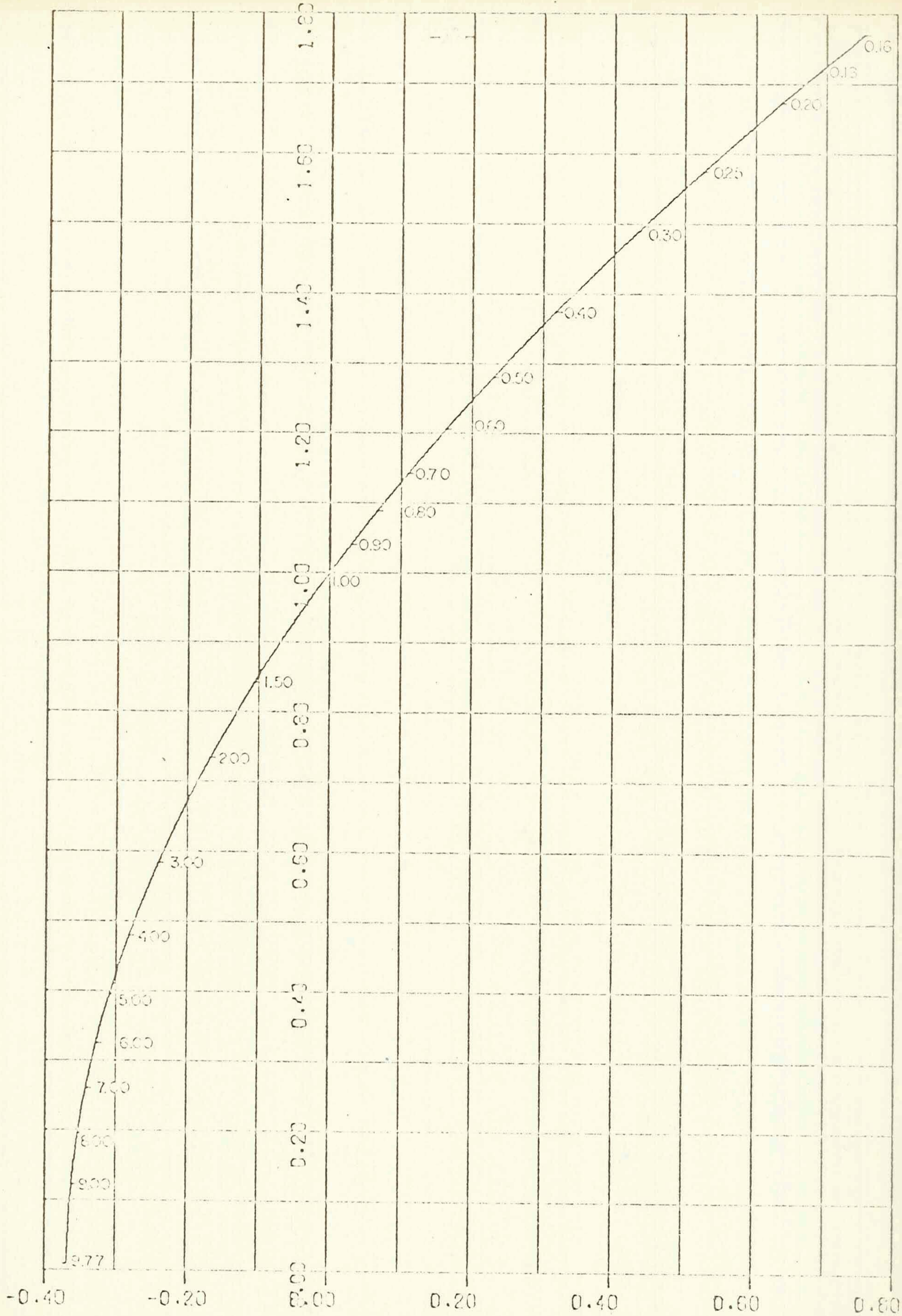

Fig. 2 Locus of dominant zero position as a function of r_f (ohms) for R_o = 17.786 ohms, C_o = 0.629 farads.

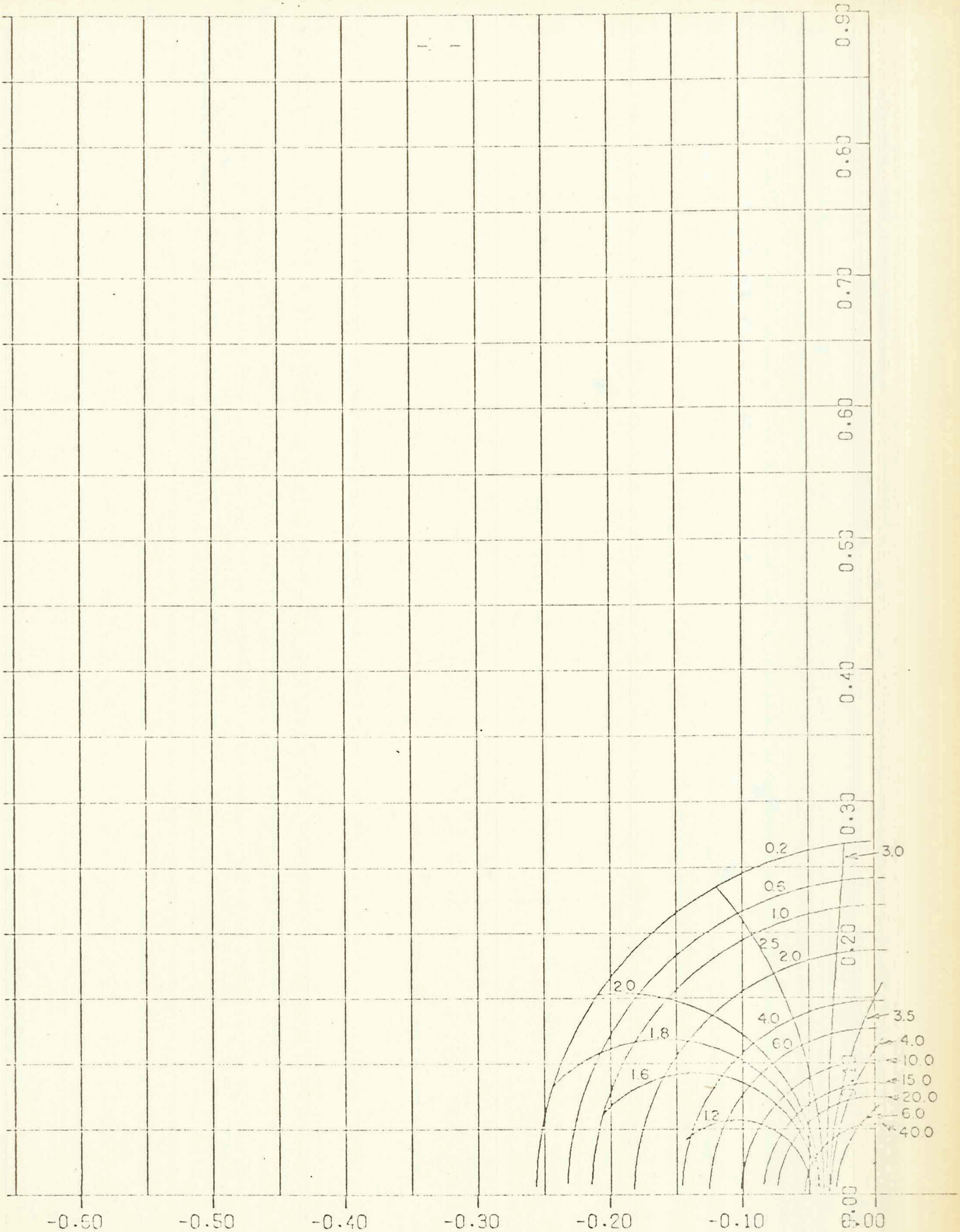

Fig. 3 Loci of dominant pole positions for C_1 = 0.7 farads.

Loci of constant r_f cover the range 0.2 - 40 ohms.

Loci of constant K cover the range 1.2 - 6.0.

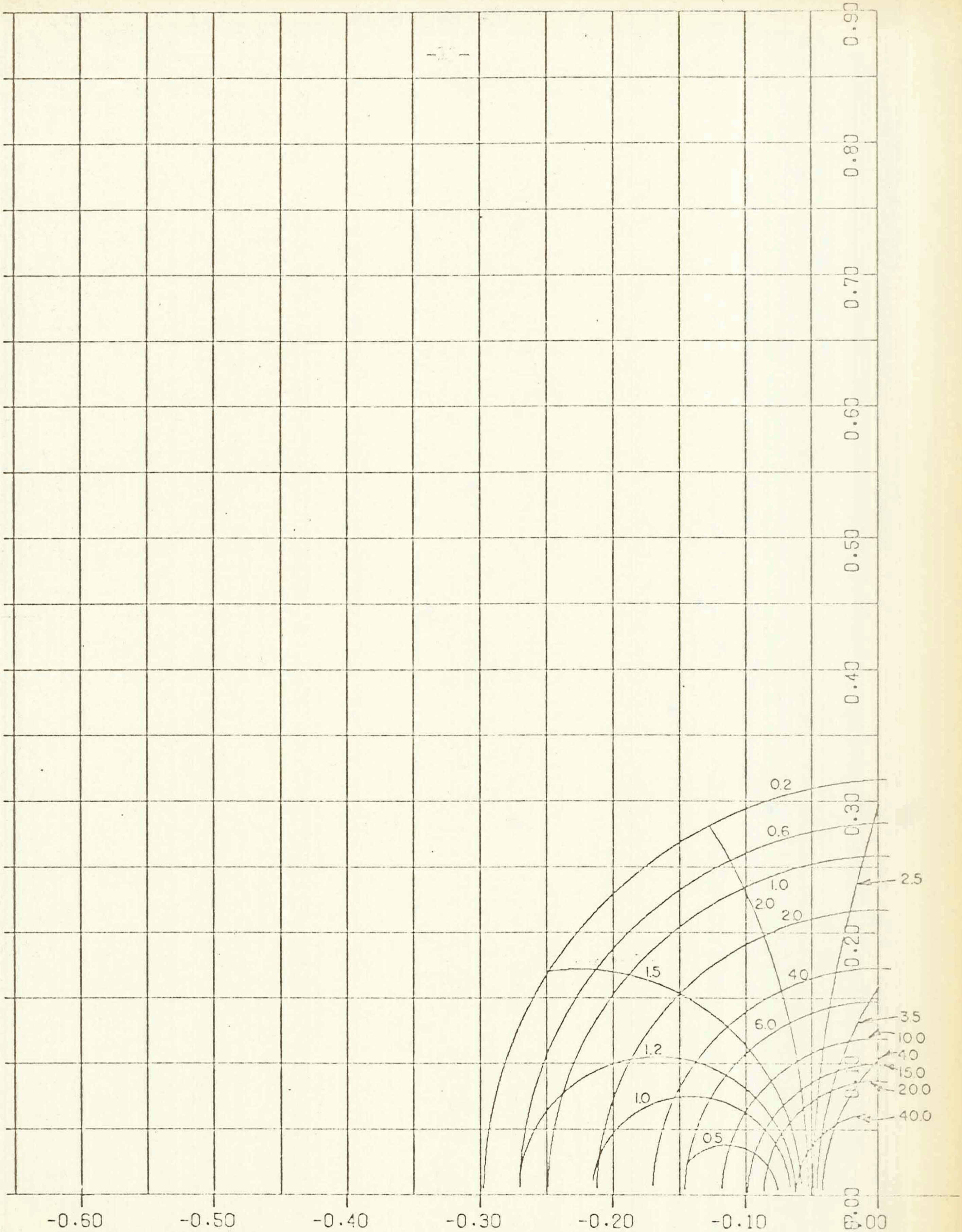

Fig. 4 Loci of dominant pole positions for $C_I = 0.5$ farads.

Loci of constant r_f cover the range 0.2 - 40 ohms.

Loci of constant K cover the range 0.5 - 4.0.

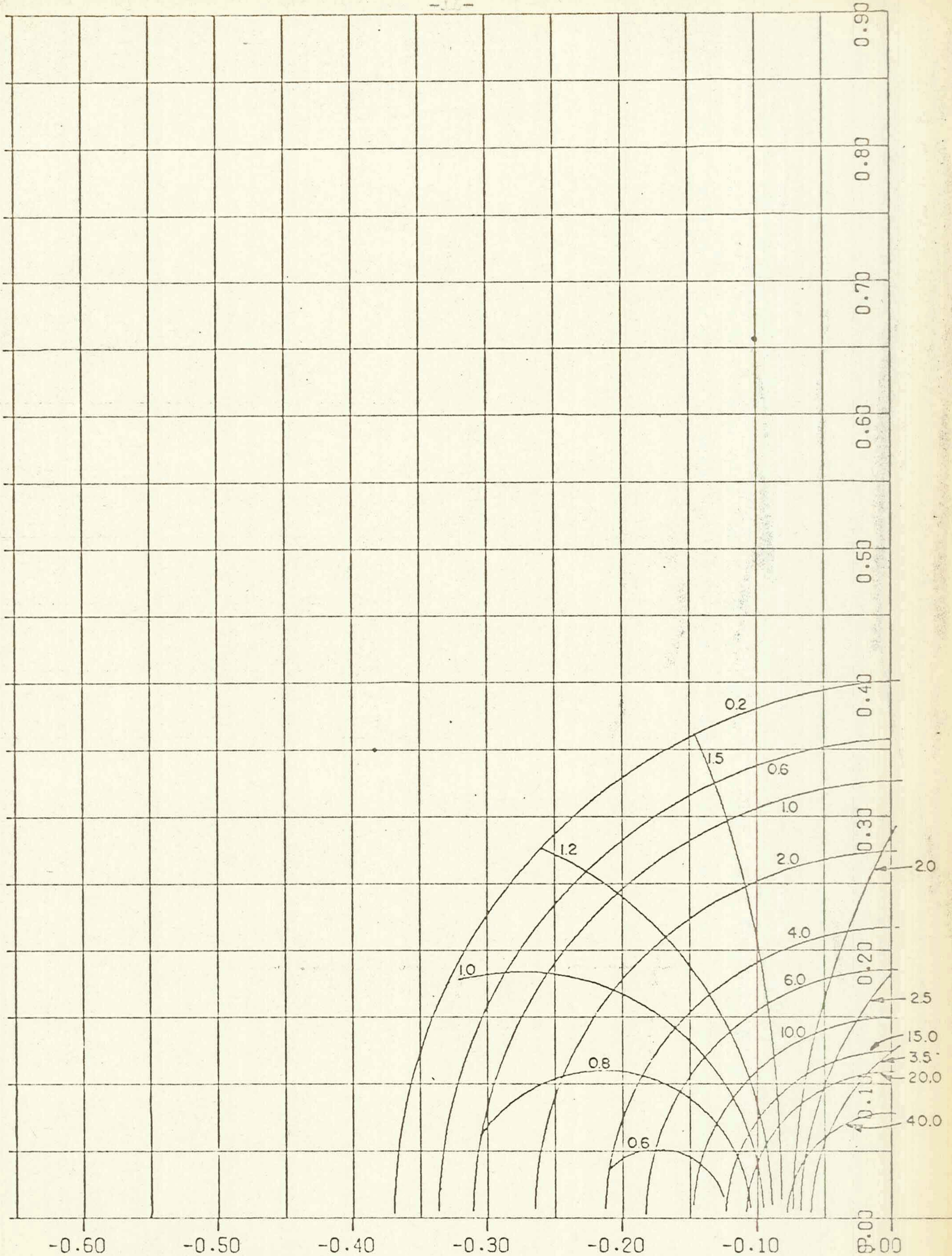

Fig. 5 Loci of dominant pole positions for $C_I = 0.3$ farads.

Loci of constant r_f cover the range 0.2 - 40 ohms.

Loci of constant K cover the range 0.6 - 3.5.

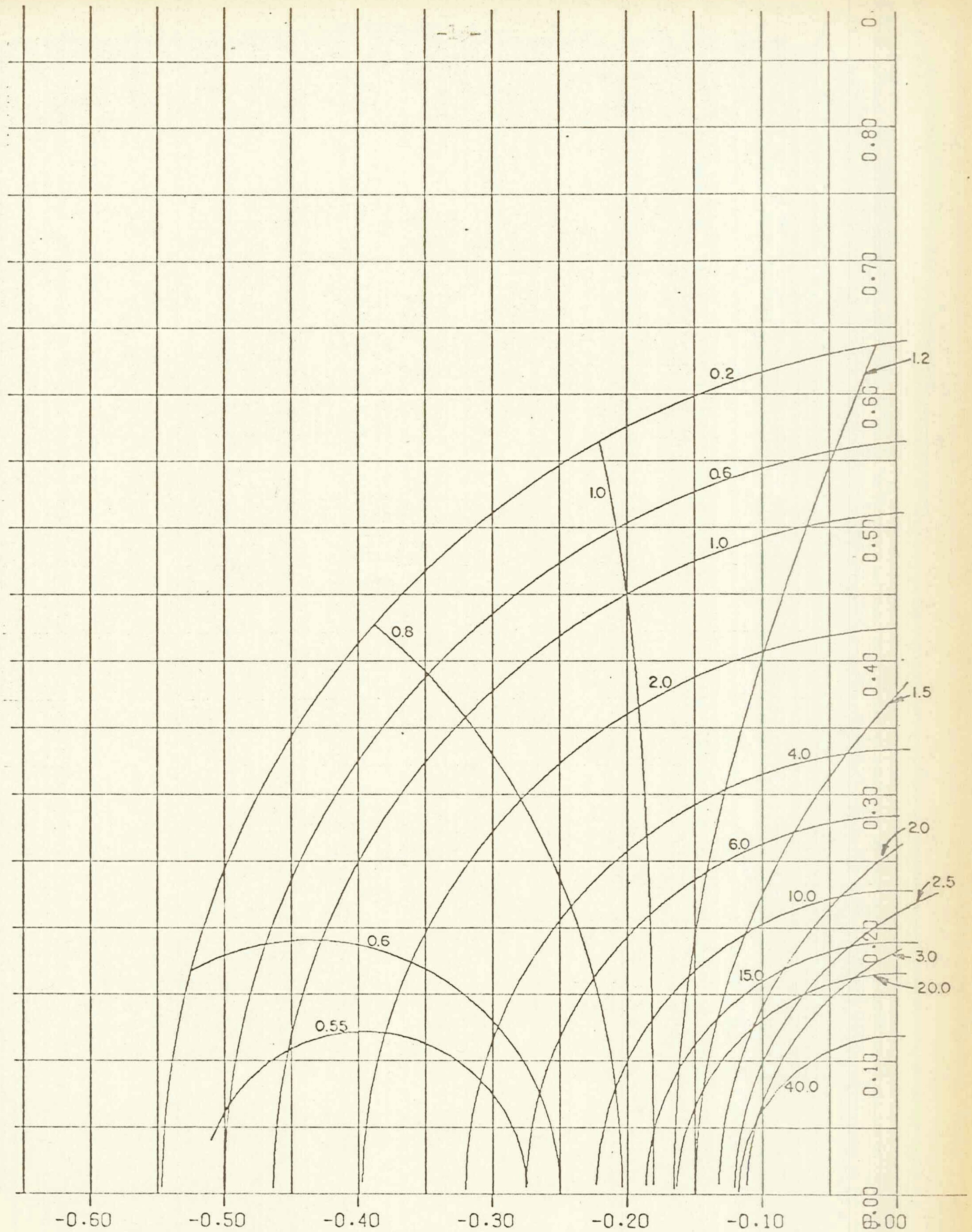

Fig. 6 Loci of dominant pole positions for C_I = 0.1 farads.
Loci of constant r_f cover the range 0.2 - 40 ohms.
Loci of constant K cover the range 0.55 - 3.0.

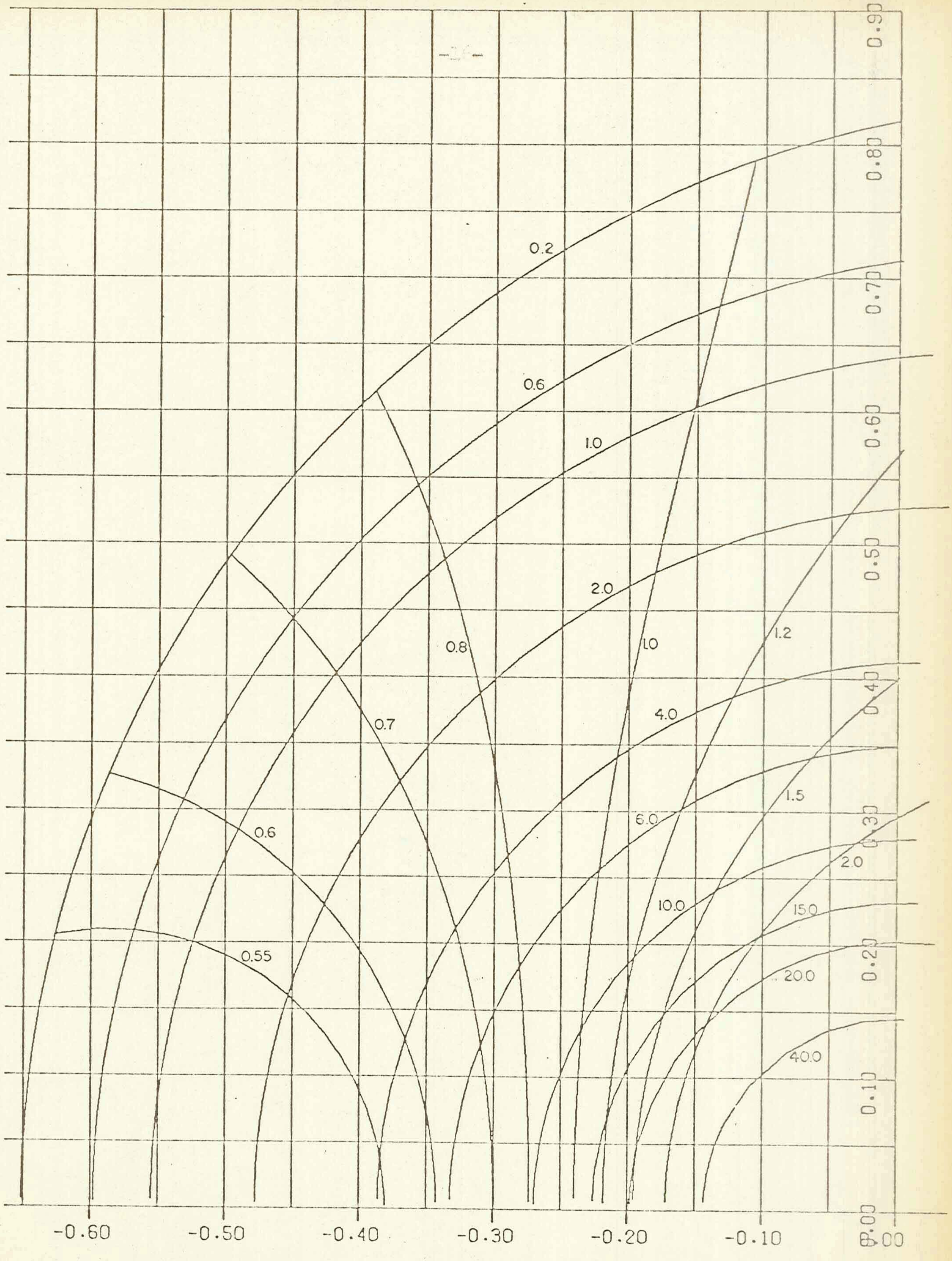

Fig. 7 Loci of dominant pole positions for C_I = 0.05 farads.

Loci of constant r_f cover the range 0.2 - 40 ohms.

Loci of constant K cover the range 0.55 - 2.

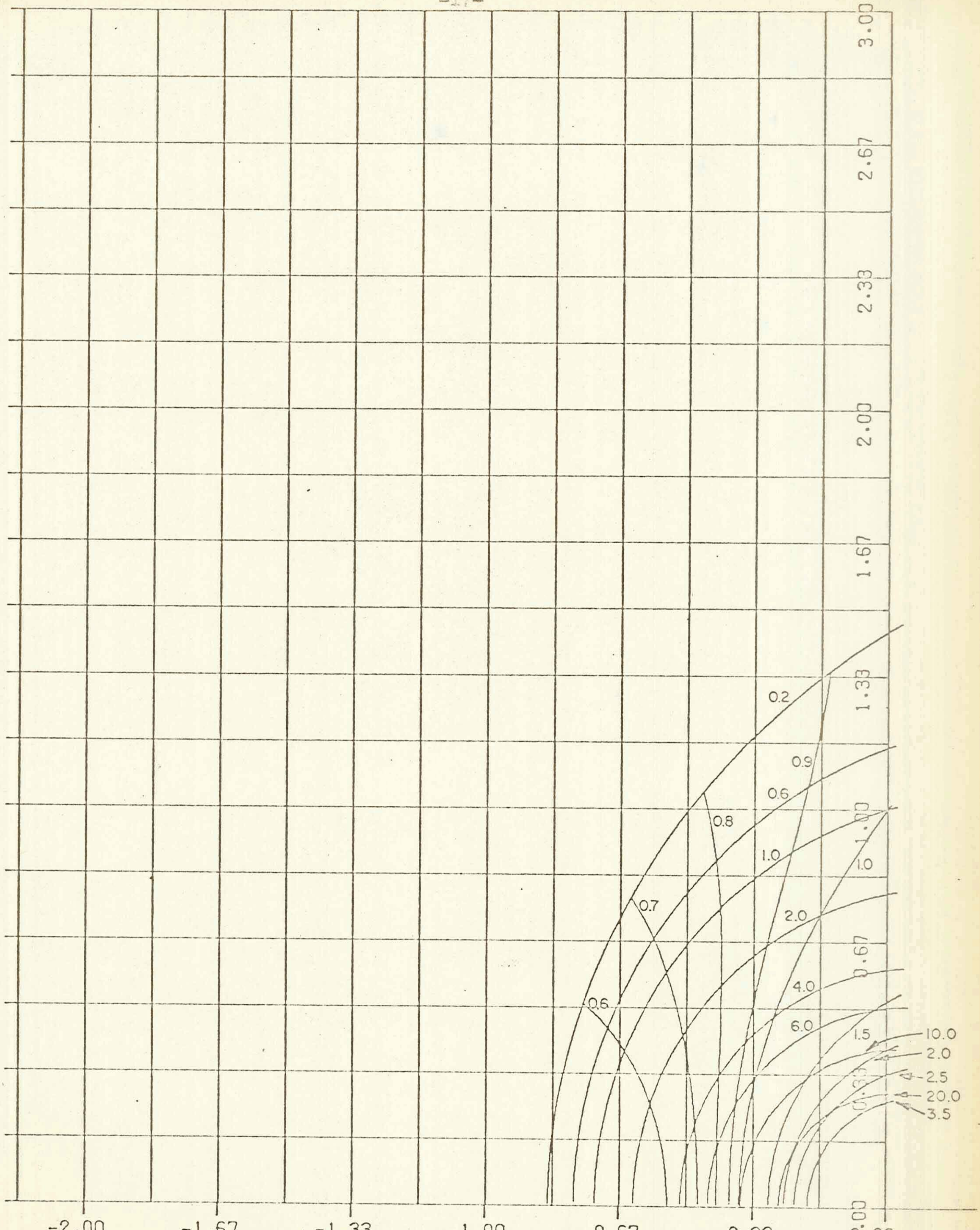

Fig. 8 Loci of dominant pole positions for $C_I = 0$ ($R_I = \infty$).
Loci of constant r_f cover the range 0.2 - 20 ohms.
Loci of constant K cover the range 0.6 - 3.5.

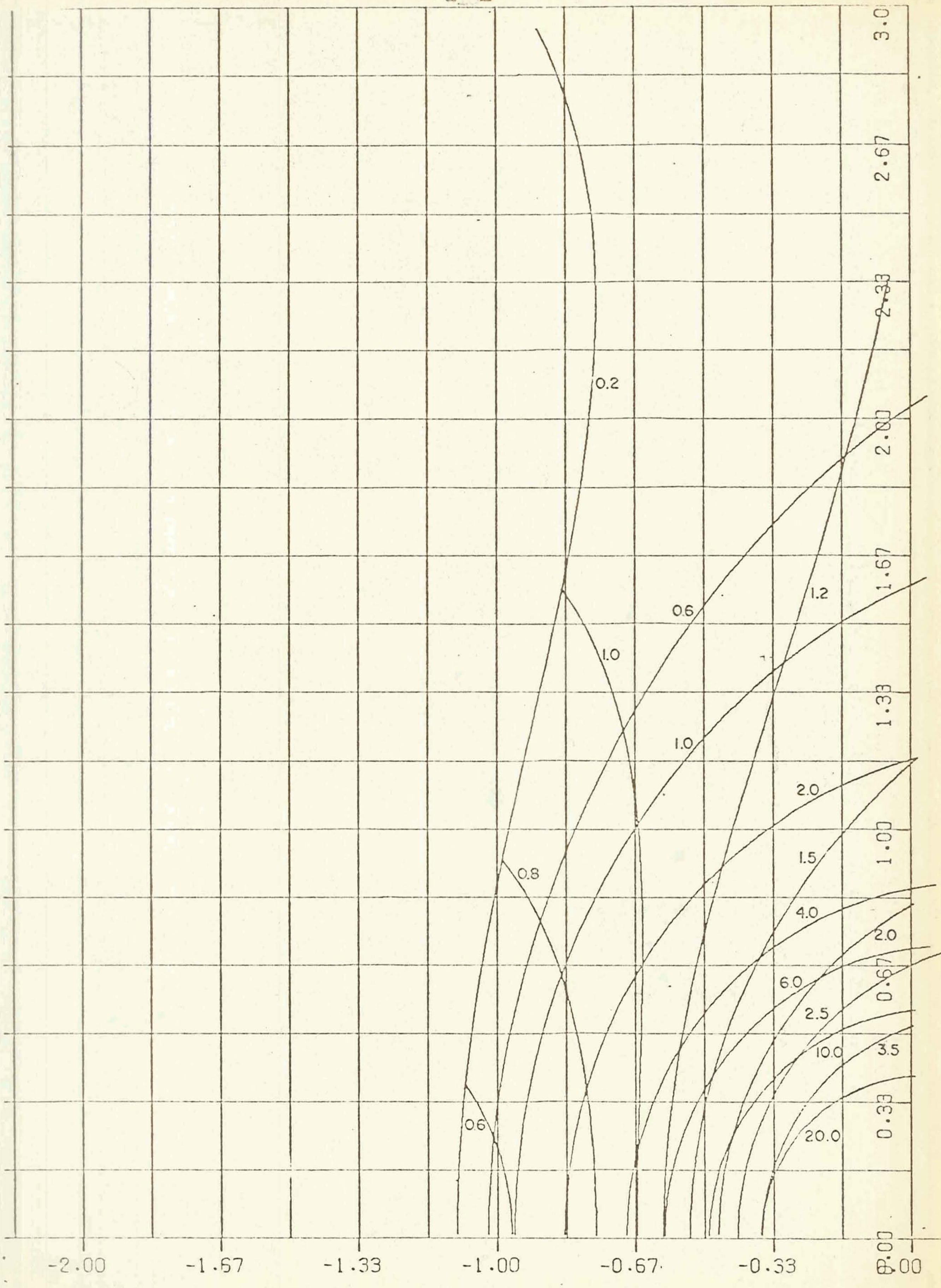

Fig. 9 Loci of dominant pole positions for R_I = 20 ohms.

Loci of constant r_f cover the range 0.2 - 20 ohms.

Loci of constant K cover the range 0.6 - 3.5.

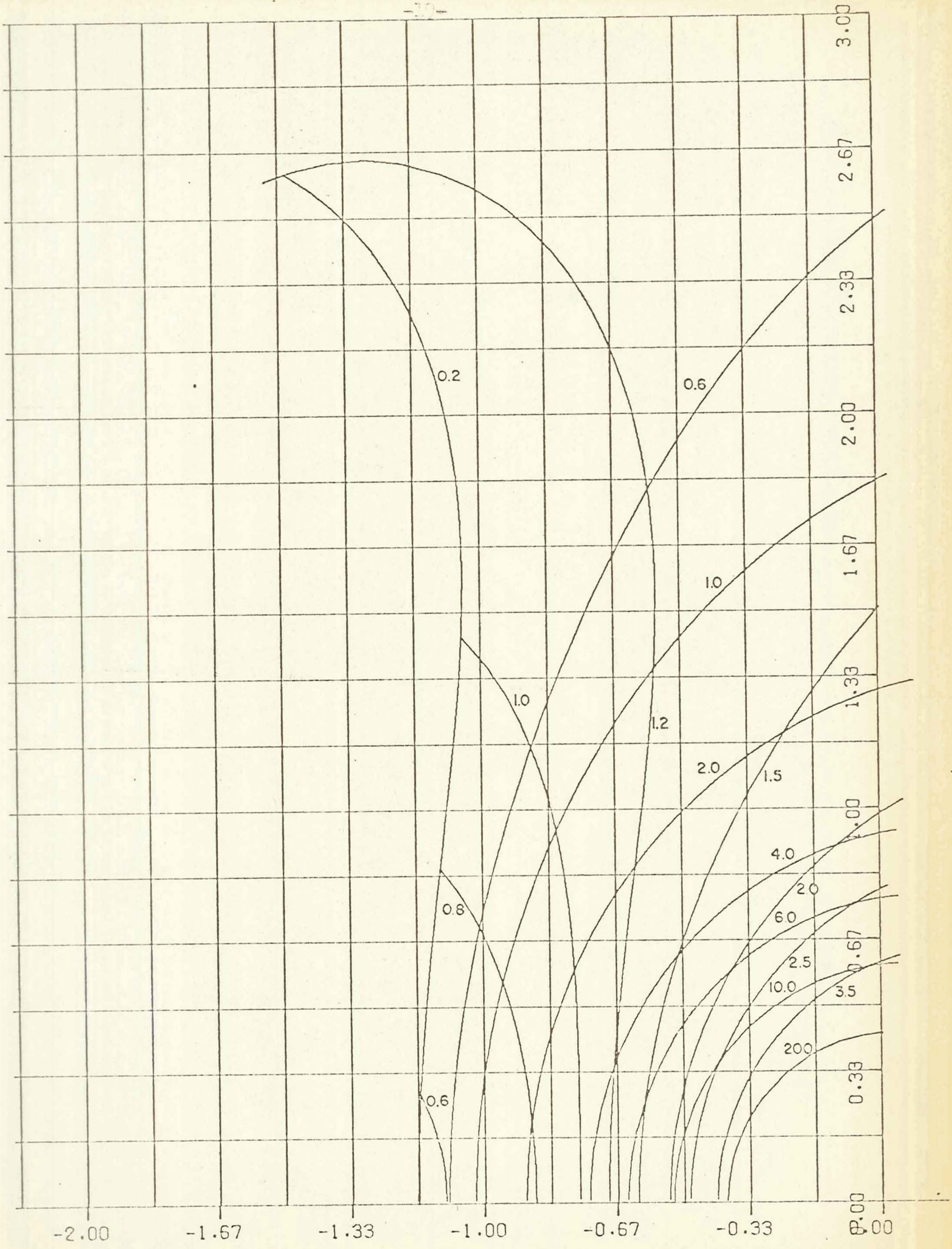

Fig. 10 Loci of dominant pole positions of R_I = 15 ohms.
Loci of constant r_f cover the range 0.2 - 20 ohms.
Loci of constant K cover the range 0.6 - 3.5.

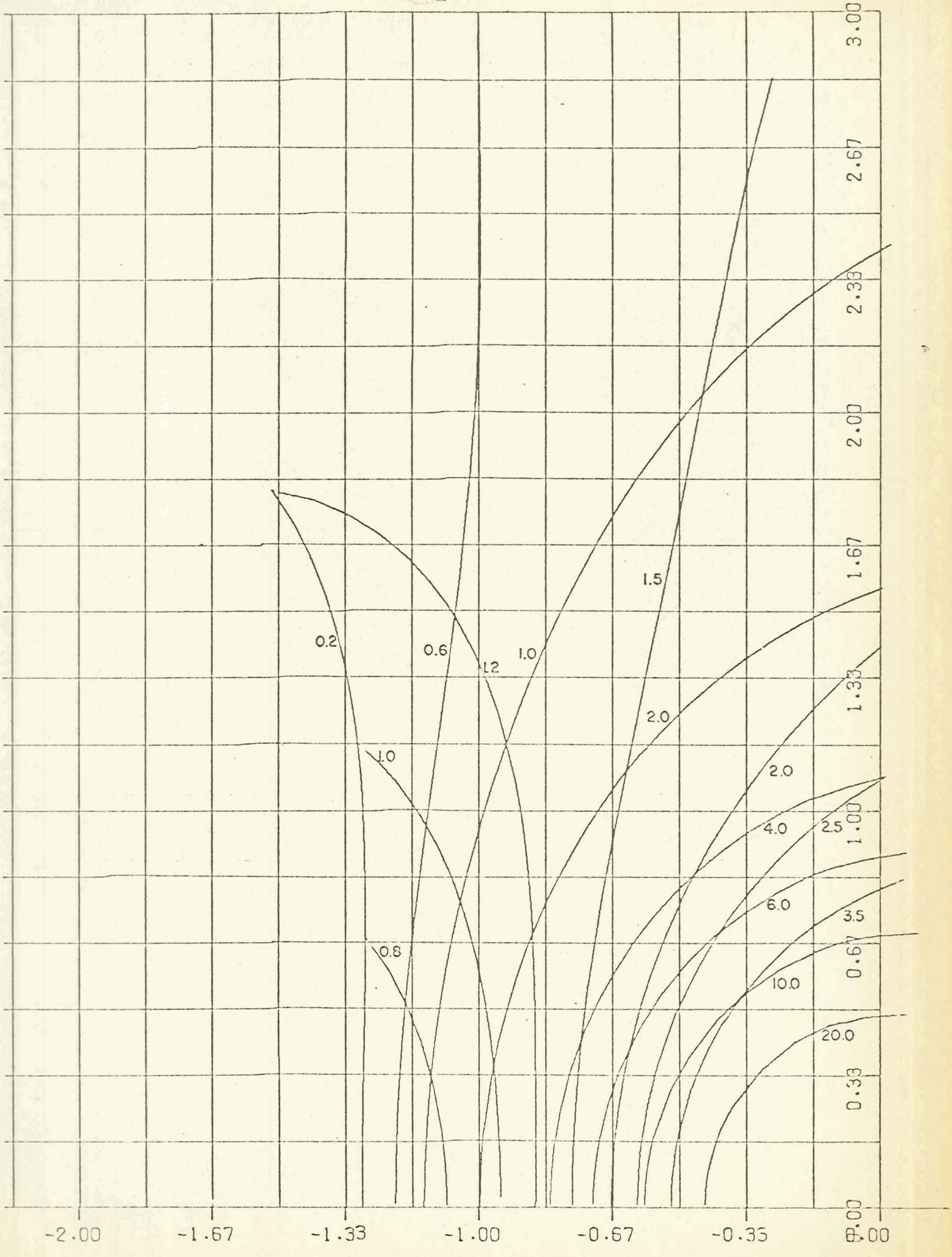

Fig. 11 Loci of dominant pole positions for R_I = 10 ohms.
Loci of constant r_f cover the range 0.2 - 20 ohms.
Loci of constant K cover the range 0.8 - 3.5.

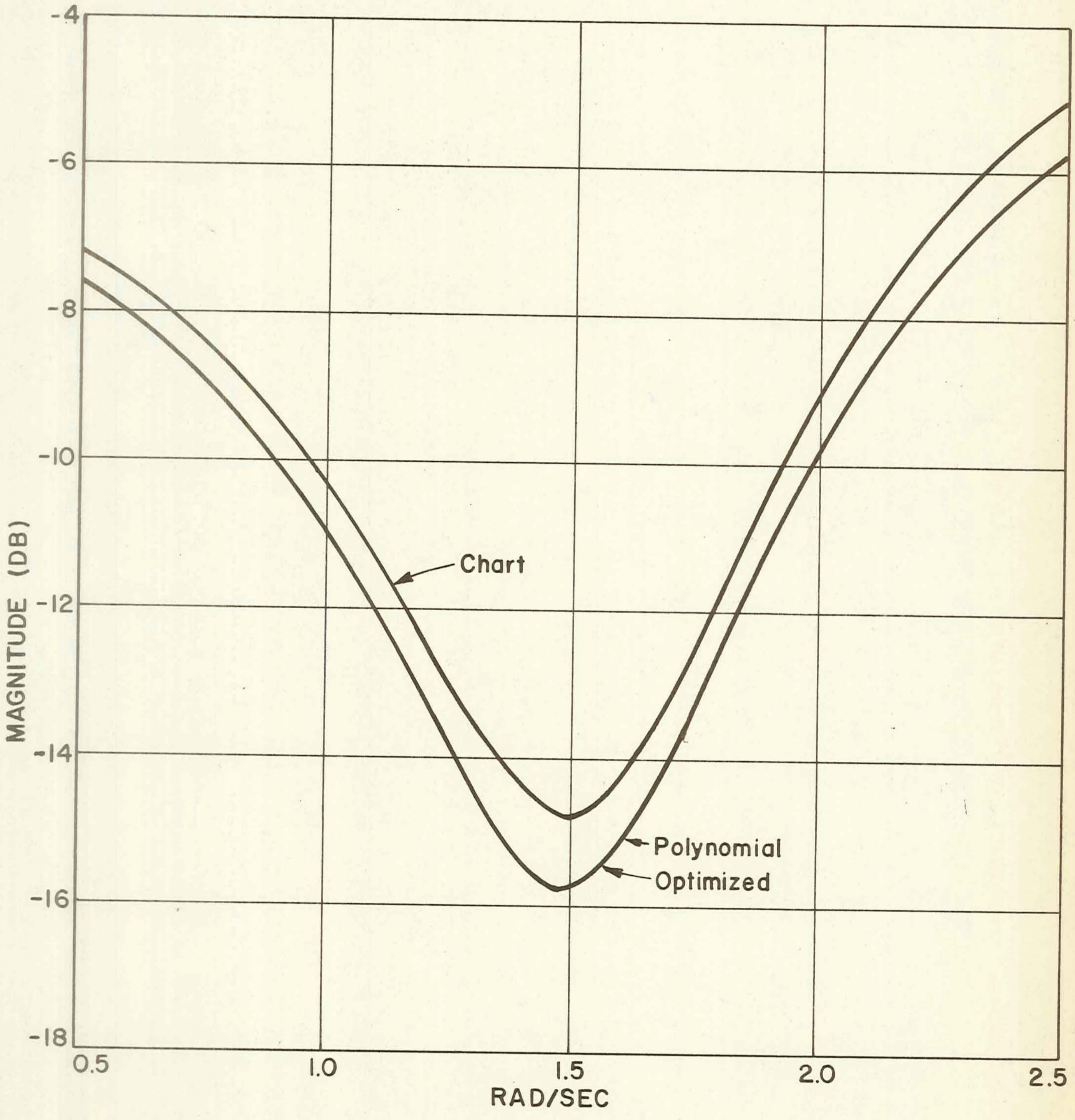

Figure 12 Magnitude characteristics for (7) and its DLA realizations.

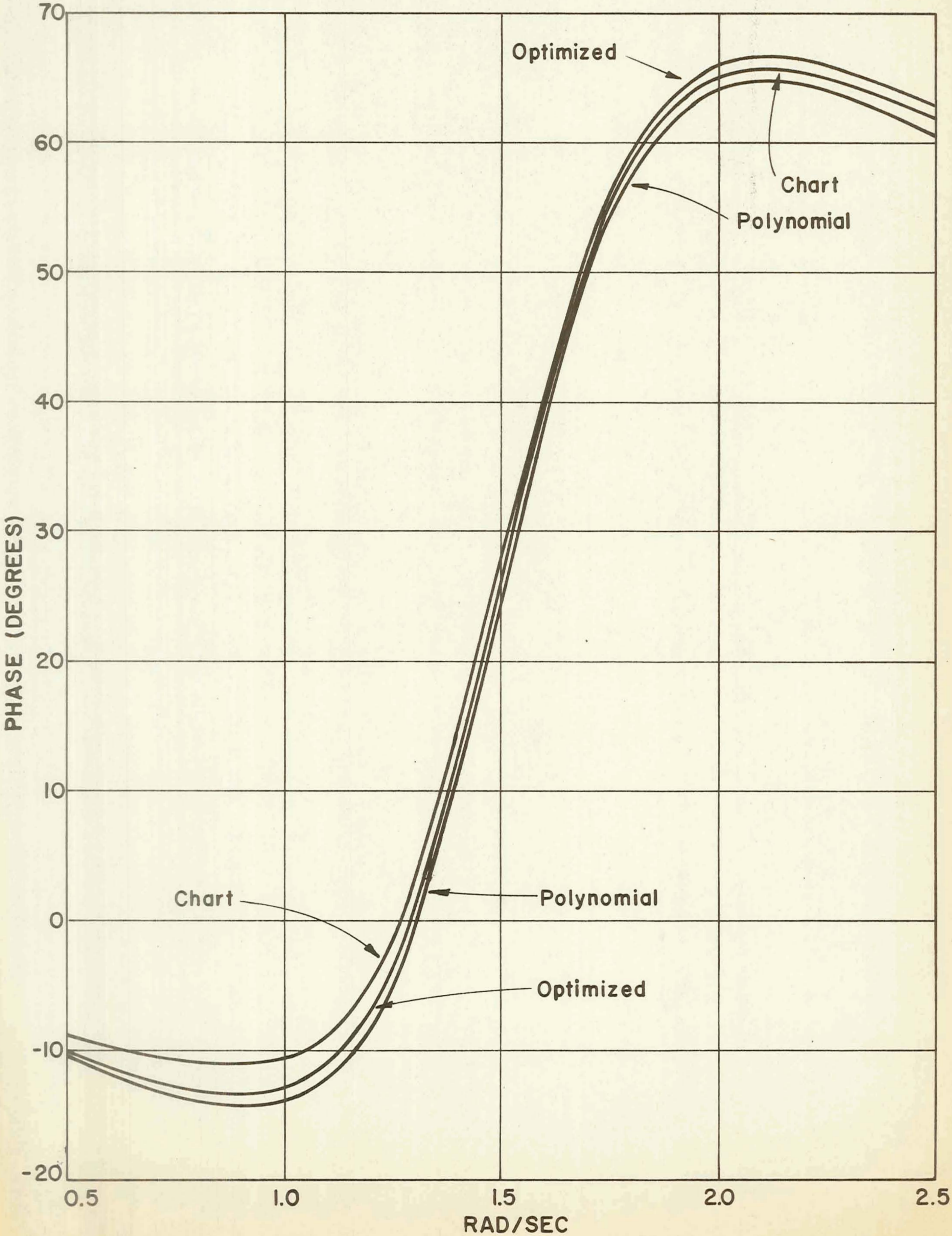

Figure 13 Phase characteristics for (7) and its DLA realizations.

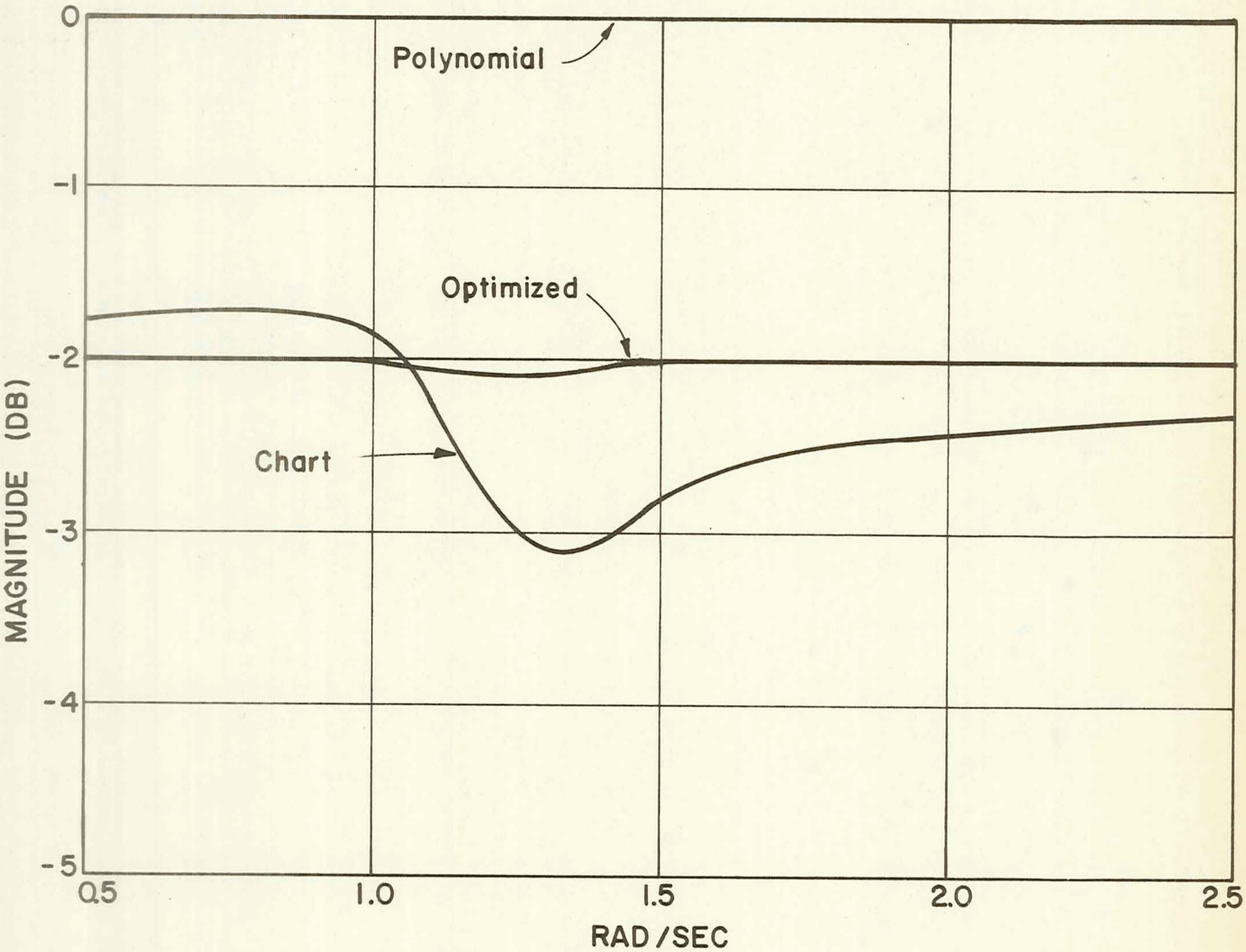

Figure 14 Magnitude characteristics for (8) and its DLA realizations.

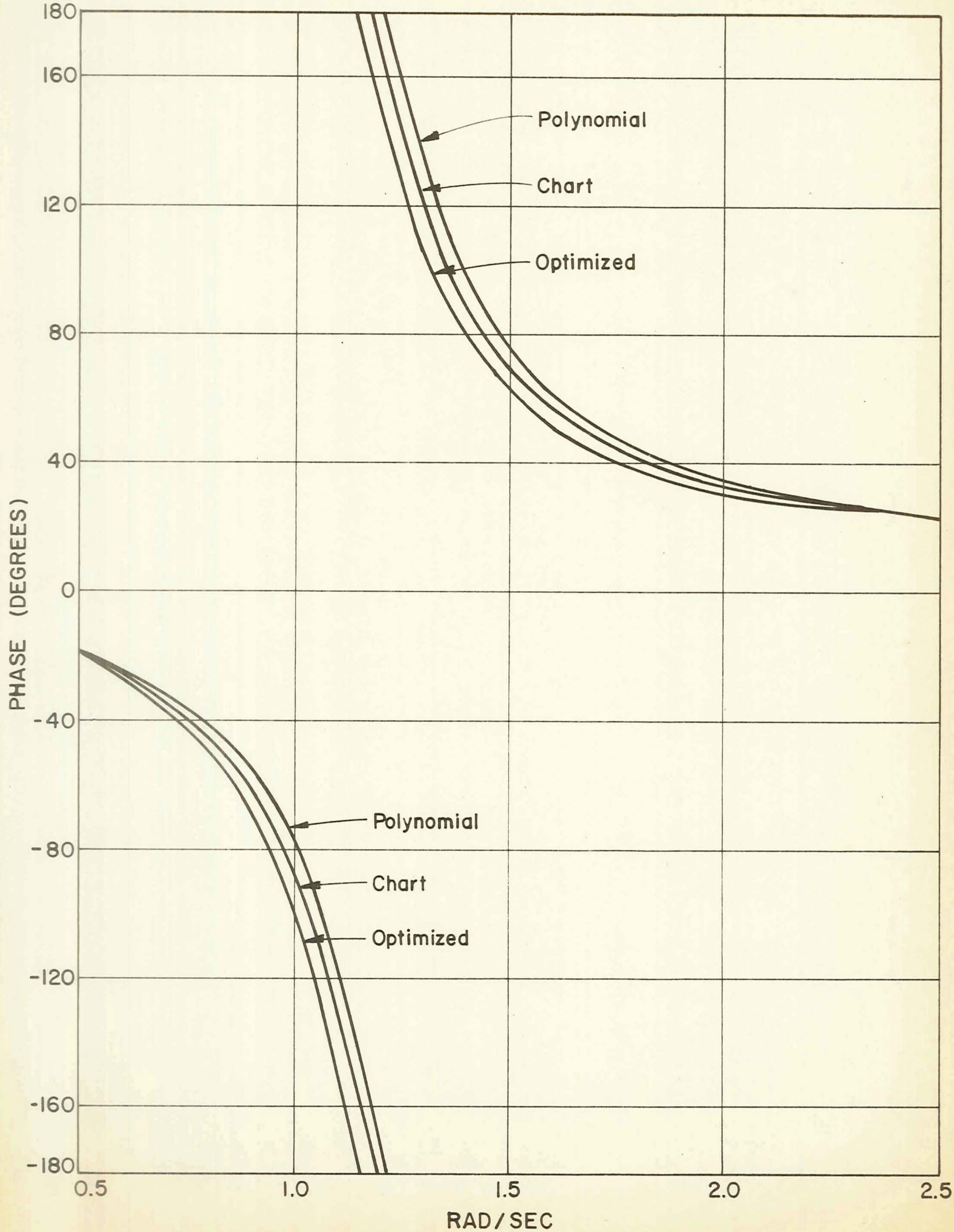

Figure 15 Phase characteristics for (8) and its DLA realizations.